



## OBSERVER BASED SLIDING MODE CONTROLLER DESIGN FOR POSITION CONTROL OF A SERVO SYSTEM HAVING UNCERTAINTIES AND DISTURBANCES

Ümit ÖNEN

Necmettin Erbakan University, Engineering Faculty, Mekatronics Engineering Department, Konya, TURKIYE  
[uonen@erbakan.edu.tr](mailto:uonen@erbakan.edu.tr)

(Geliş/Received: 14.04.2022; Kabul/Accepted in Revised Form: 16.06.2022)

**ABSTRACT:** Servo systems are used extensively in many industrial applications that require precise position control. However, parameter uncertainties, matched and unmatched disturbances encountered in most of these applications adversely affect the controller performance. Therefore, in industrial control applications, robustness is at least as important as precision. In this study, an Extended State Observer-based Sliding Mode Controller (GDGKKK) design is presented for precise position control of a rotary servo system having parameter uncertainties and disturbance input. The performance of the proposed controller has been tested by performing simulation studies for five different uncertainty and disturbance input scenarios and compared with the traditional Sliding Mode Control (SMC) and Proportional Derivative (PD) control to evaluate its effectiveness. The mathematical model of the Quanser SRV02 rotary servo unit was used in the simulation studies in MATLAB/Simulink software. The simulation results show that the PD control is very sensitive to load changes and disturbances and while the traditional SMC control is insensitive to load changes and matched disturbances, it is sensitive to mismatched disturbances. On the other hand, the results clearly showed that the proposed GDGKKK controller offers extremely successful disturbance rejection performance against both load changes and matched and unmatched disturbances.

**Keywords:** Observer, Robust Control, Sliding Mode Control (SMC), Position Control, Servomotor

### Belirsizlik ve Bozuculara Sahip Bir Servo Sistemin Konum Kontrolü İçin Gözlemci Tabanlı Kayan Kipli Kontrolcü Tasarımı

**ÖZ:** Servo sistemler, hassas konum kontrolü gerektiren birçok endüstriyel uygulamada yoğun olarak kullanılmaktadır. Ancak bu uygulamaların çoğunda karşılaşılan parametre belirsizlikleri, eşleşen ve eşleşmeyen bozucu etkenler, kontrolcü performansını olumsuz yönde etkilemektedir. Dolayısıyla endüstriyel kontrol uygulamalarında gürbüzlukte en az hassasiyet kadar önem taşımaktadır. Bu çalışmada, parametre belirsizlikleri ve bozucu girişe sahip bir döner servo sistemin hassas pozisyon kontrolü için Genişletilmiş Durum Gözlemcisine dayalı Kayan Kipli Kontrolcü (GDGKKK) tasarımı sunulmuştur. Önerilen kontrolcünün performansı, beş farklı belirsizlik ve bozucu giriş senaryosu için benzetim çalışmaları yapılarak test edilmiş ve etkinliğinin değerlendirilebilmesi için klasik Kayan Kipli Kontrol (SMC) ve Oransal Türevsel (PD) kontrol ile kıyaslanmıştır. MATLAB/Simulink yazılımında benzetim çalışmalarında Quanser SRV02 döner servo ünitesine ait matematiksel model kullanılmıştır. Benzetim sonuçları, PD kontrolün yük değişimlerine ve bozucu girişlere karşı oldukça duyarlı olduğunu, klasik SMC kontrolün ise yük değişimleri ve eşleşen bozuculara karşı dayanıklı olmakla birlikte eşleşmeyen bozuculara karşı duyarlı olduğunu göstermiştir. Diğer yandan sonuçlar, önerilen GDGKKK kontrolcünün hem yük değişimlerine hem de eşleşen ve eşleşmeyen bozuculara karşı son derece başarılı bir bozucu reddetme performansı sunduğunu açıkça göstermiştir.

**Anahtar Kelimeler:** Gözlemci, Gürbüz Kontrol, Kayan Kipli Kontrol (KKK), Konum kontrolü, Servomotor

## 1. INTRODUCTION

Servo systems are widely used in many fields of industry, especially in applications requiring precise motion control due to their advantages such as light weight and small structure, high performance and efficiency, high torque/inertia ratio, reliability and low noise. Traditional PID control has been used intensively in servo motor control due to its simple structure and easy application. The PID controller can guarantee a robust and suitable control performance if an accurate dynamic model and detailed information about the disturbances can be obtained (Cheon *et al.*, 2004). However, in most practical applications, servo systems have kinds of disturbances and uncertainties because of nonlinear friction, measurement noise, load variations, external disturbances, etc. (Wang *et al.*, 2017). The presence of the system uncertainties, parameter changes and external disturbances results in poor control performance for conventional linear control methods.

In recent years, researchers have focused on servo systems affected by uncertainties and disturbances and they have proposed many different control methods to increase the robustness of the systems. Among all these control methods, SMC has stand out as one of the most effective methods in terms of robustness due to its invariance property against the external disturbances and parameter variations. SMC uses a discontinuous control action to force the state trajectories of the system to a predefined sliding surface. After the system states reach the sliding surface, the stability and dynamic characteristics of the system is independent of certain perturbations including external disturbances and only depend on the sliding surface parameters.

Although the SMC provides fast response and good robustness features, it has some disadvantages such as chattering and sensitivity to mismatched disturbances. Chattering is the high frequency oscillations that occur near the sliding surface due to the discontinuous control law. In addition to decreasing control performance, chattering can cause actuator failure in practical applications. Researchers have proposed many methods for eliminating or reducing the effect of chattering. A novel exponential reaching law for the conventional SMC was presented in (Wang *et al.*, 2013), a boundary layer around the switching surface which replace the discontinuous control law with a continuous one is used in (Kachroo and Tomizuka, 1996; Baik *et al.*, 2000), second order and higher-order SMC methods are used in (Bartolini *et al.*, 1998; Levant, 2003) and low-pass filtering is used in (Tseng and Chen, 2010). Fuzzy-logic based SMC (Ha *et al.*, 2001) and Nonsingular Terminal SMC (Zheng *et al.*, 2014) are some other methods proposed to avoid chattering by using continuous functions instead of classical switching functions. In order to ensure robustness, the switching gain must be selected to be greater than the upper bound of the disturbance. But in most of the practical applications, it is difficult to measure or estimate the upper bound of the disturbance and so the switching gain could be much large. Because of the large switching gain cause large chattering, adaptive SMC and neural-network based SMC methods are used to tune proper switching gains in (Bao *et al.*, 2010; Wang *et al.*, 2009).

Besides the chattering phenomenon, the most of the existing traditional SMC approaches are insensitive only to matched disturbances and cannot attenuate mismatched disturbances which act in a different channel than the control input, effectively. Some researchers have proposed integral SMC and global SMC methods in (Rubagotti *et al.*, 2011; Liu *et al.*, 2014) to improve the disturbance rejection performance of the SMC for the systems effected of matched and mismatched disturbances. Some researchers have combined SMC control with other robust control techniques such as backstepping in (Li and Hu, 2011) and adaptive control in (Chang, 2009).

On the other hand, disturbance observer-based SMC is one of the most effective approach used to deal with mismatched disturbances. Besides increasing the robustness, it can also reduce the chattering since the switching gain can be reduced to small values after the disturbance is estimated and compensated in control input.

In (Cheon *et al.*, 2004) a disturbance estimator-based SMC controller was proposed for position control of AC servomotor subjected to external disturbance, in (Shao *et al.*, 2021) recursive SMC combined with an adaptive disturbance observer was used for position control of a linear motor deteriorated by payload variations, friction and external disturbances, a nonlinear disturbance observer-based SMC was used for

systems with matched and mismatched uncertainties in (Hou *et al.*, 2017). A SMC based on an unknown system dynamics estimator was proposed in (Wang *et al.*, 2020) for a servomechanism having unknown system dynamics. A nonlinear disturbance observer based terminal SMC was proposed for nonlinear systems subjected to both matched and mismatched disturbances in (Nguyen *et al.*, 2021) and Extended state observer-based SMC was used for a class of nonlinear systems subjected to matched and mismatched disturbance in (Shi *et al.*, 2018). All these studies show that the disturbance observers reduce the chattering problem as well as increasing the disturbance rejection property of the SMC control effectively.

In this study ESO based SMC control of a rotary servo system having parameter uncertainties and disturbances is realized. While traditional SMC control is a robust control method against parameter changes and matched disturbances, it is sensitive to mismatched disturbances. So, in the proposed control scheme, an ESO was added to the control scheme to improve the disturbance rejection capability of the SMC control against mismatched disturbances. The performance of the proposed controller was tested on simulation model of Quanser SRV02 servo unit for five different conditions consisted of different uncertainties and disturbances and compared with the traditional SMC and PD control in order to evaluate its effectiveness. The results showed that the proposed ESOSMC controller provided much better performance against load variations, matched and mismatched disturbances compared to both PD and traditional SMC control.

## 2. MATHEMATICAL MODEL OF THE ROTARY SERVO SYSTEM

In this study, mathematical model of SRV02 rotary servo base unit of Quanser Inc. was used as simulation model. Schematic of the DC motor armature circuit and the gearbox of the SRV02 is shown in Fig. 1.

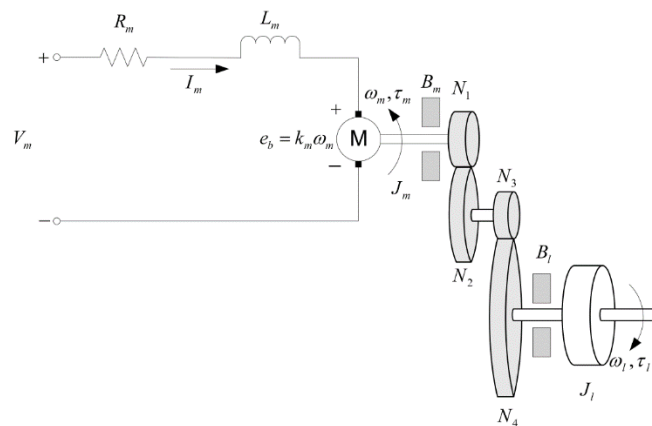


**Figure 1.** Armature circuit and gear train of the SRV02 rotary servo system

The equation of the armature circuit can be obtained by using Kirchoff's Voltage Law as

$$V_m(t) - R_m I_m(t) - k_m \omega_m(t) = 0 \quad (1)$$

where  $V_m(t)$ ,  $R_m$  and  $I_m(t)$  is the input voltage, armature resistance and armature current of the motor respectively,  $\omega_m(t)$  is the angular velocity of the motor shaft and  $k_m$  is the back-emf constant of the motor. Motor inductance  $L_m$  is neglected since it is much less than resistance. The equation of motion of the load can be derived by using Newton's Second Law of Motion as

$$J_l \frac{d\omega_l(t)}{dt} + B_l \omega_l(t) = \tau_l(t) \quad (2)$$

where  $J_l$  is the moment of inertia of the load which includes the inertia of the gearbox and the inertia of the attached external loads,  $B_l$  is the viscous friction coefficient of the load shaft,  $\omega_l(t)$  is the angular velocity of the load shaft and  $\tau_l(t)$  is the total torque applied on the load. The equation of motion of the motor shaft can be written as follows by the same way,

$$J_m \frac{d\omega_m(t)}{dt} + B_m \omega_m(t) + \tau_{ml}(t) = \tau_m(t) \quad (3)$$

where  $J_m$  is the moment of inertia of the motor shaft,  $B_m$  is the viscous friction acting on the motor shaft,  $\tau_{ml}(t)$  is the resulting torque acting on the motor shaft from the load torque and  $\tau_m(t)$  is the total motor torque. The resulting torque  $\tau_{ml}(t)$  transferred from the load torque to the motor shaft can be found as follows.

$$\tau_{ml}(t) = \frac{\tau_l(t)}{\eta_g K_g} \quad (4)$$

where  $\eta_g$  is the gearbox efficiency and  $K_g$  is the gear ratio. The relationships between the positions and angular velocities of the load and motor shaft can be defined as follows.

$$\theta_m(t) = K_g \theta_l(t) \quad (5)$$

$$\omega_m(t) = K_g \omega_l(t) \quad (6)$$

Equation of motion of the load shaft with respect to applied motor torque can be obtained by substituting Eq. 2, 4 and 6 into Eq. 3 as follows.

$$J_{eq} \frac{d\omega_l(t)}{dt} + B_{eq} \omega_l = \eta_g K_g \tau_m(t) \quad (7)$$

In this equation, the equivalent moment of inertia  $J_{eq}$  and the equivalent damping coefficient of the motor  $B_{eq}$  can be defined as,

$$J_{eq} = \eta_g K_g^2 J_m + J_l \quad (8)$$

$$B_{eq} = \eta_g K_g^2 B_m + B_l \quad (9)$$

The relationship between the motor torque and the current can be defined as

$$\tau_m(t) = \eta_m k_t I_m(t) \quad (10)$$

where  $k_t$  is the current-torque constant and  $\eta_m$  is the motor efficiency. The motor torque can be expressed with respect to the input voltage  $V_m(t)$  and the angular velocity of the load shaft  $\omega_l(t)$  by subtracting  $I_m(t)$  from Eq. (1) and substituting it in Eq. (10).

$$\tau_m(t) = \frac{\eta_m k_t (V_m(t) - k_m K_g \omega_l(t))}{R_m} \quad (11)$$

If we substitute Eq. (11) into Eq. (7), we can obtain the expression of the angular velocity of the load shaft with respect to input voltage,

$$J_{eq} \left( \frac{d}{dt} \omega_l(t) \right) + B_{eqv} \omega_l(t) = A_m V_m(t) \tag{12}$$

In this equation the total equivalent damping term  $B_{eqv}$  and the actuator gain  $A_m$  can be defined as follows.

$$B_{eqv} = \frac{\eta_g K_g^2 \eta_m k_t k_m + B_{eq} R_m}{R_m} \tag{13}$$

$$A_m = \frac{\eta_g K_g \eta_m k_t}{R_m} \tag{14}$$

In most of the practical applications of the electromechanical systems have parameter uncertainties and disturbances because of the mass variations, actuator saturation, external forces, damping, friction, sensor noises, etc. So, the system defined in Eq. (12) can be considered as

$$\ddot{\theta}_l = f(\theta, t) + \alpha u(t) + d(t) \tag{15}$$

where  $\theta_l(t)$  is the load shaft angle,  $u(t)$  is the control signal,  $\alpha$  is a constant,  $f(\theta, t)$  is a function of  $\theta_l(t)$  and  $d(t)$  is sum of the disturbance and uncertainty of the system. We assume that the total disturbance is bounded and  $|d(t)| \leq D$ . By defining the states and the outputs of the system as  $\mathbf{x}(t) = [x_1(t) \ x_2(t)]^T = [\theta_l(t) \ \dot{\theta}_l(t)]^T$  and  $\mathbf{y} = [y_1 \ y_2]^T = [x_1 \ x_2]^T$  respectively, the system given in Eq. (15) can be written as follows.

$$\begin{aligned} \dot{x}_1(t) &= x_2(t) \\ \dot{x}_2(t) &= f(\theta, t) + \alpha u(t) + d(t) \end{aligned} \tag{16}$$

### 3. SLIDING MODE CONTROL OF THE SERVO SYSTEM

Traditional SMC control scheme of the servo system is given in Fig. 2. The SMC control law consist of two parts as equivalent control and switching control. The equivalent control drives the system states to sliding surface and the switching control keeps the system states on the sliding surface.

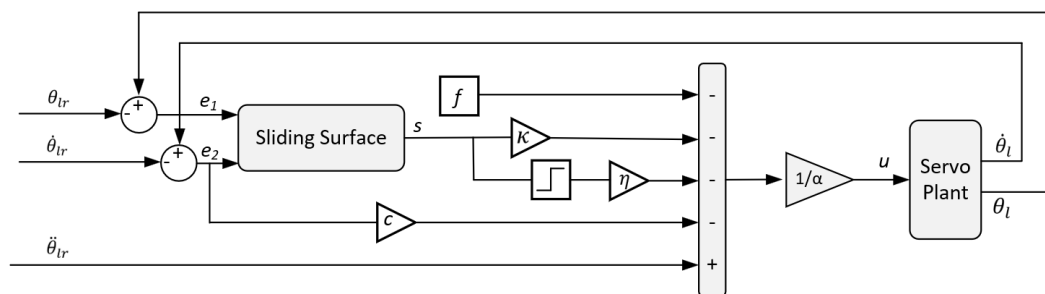


Figure 2. Traditional SMC control scheme

The total control input of the SMC is defined as;

$$u(t) = u_{eq}(t) + u_{sw}(t) \tag{17}$$

where  $u_{eq}(t)$  denotes the equivalent control and  $u_{sw}(t)$  denotes the switching control. In order to obtain equivalent control signal  $u_{eq}(t)$ , the plant is described as below by ignoring the external disturbance and uncertainty.

$$\begin{aligned}\dot{x}_1(t) &= x_2(t) \\ \dot{x}_2(t) &= f(\theta, t) + \alpha u(t)\end{aligned}\quad (18)$$

If the desired load shaft angle is denoted by  $\theta_{lr}$ , the state error can be defined as  $e_1(t) = \theta_l(t) - \theta_{lr}$ . So, the error system can be written as

$$\begin{aligned}\dot{e}_1(t) &= e_2(t) \\ \dot{e}_2(t) &= f(\theta, t) - \ddot{\theta}_{lr} + \alpha u(t)\end{aligned}\quad (19)$$

Sliding surface can be selected as,

$$s(t) = c e_1(t) + e_2(t)\quad (20)$$

where,  $c > 0$  is a positive constant. Derivative of the sliding surface can be obtained as

$$\dot{s}(t) = c \dot{e}_1(t) + \dot{e}_2(t) = c e_2(t) + f(\theta, t) - \ddot{\theta}_{lr} + \alpha u(t)\quad (21)$$

The equivalent control signal can be found by setting the derivative of the sliding surface equals to zero.

$$u_{eq}(t) = \frac{1}{\alpha} (\ddot{\theta}_{lr} - f(\theta, t) - c e_2(t))\quad (22)$$

Lyapunov function can be selected as,

$$V(t) = \frac{1}{2} s(t)^2\quad (23)$$

According to Lyapunov stability theory, reaching condition of the sliding mode can be defined as

$$\dot{V}(t) = s(t)\dot{s}(t) < 0\quad (24)$$

In order to satisfy the reaching condition, the switching control can be chosen as below by using exponential reaching law.

$$u_{sw}(t) = -\frac{1}{\alpha} (\kappa s(t) + \eta \operatorname{sgn}(s(t)))\quad (25)$$

where,  $\kappa$  and  $\eta$  are positive constants. Thus, total control input can be obtained by using Eq. (17) as

$$u = \frac{1}{\alpha} (\ddot{\theta}_{lr} - f(\theta, t) - c e_2(t) - \kappa s(t) - \eta \operatorname{sgn}(s(t)))\quad (26)$$

### Stability Proof:

Derivative of the sliding surface can be written as

$$\dot{s}(t) = c \dot{e}_1(t) + \dot{e}_2(t) = c e_2(t) + f(\theta, t) - \ddot{\theta}_{lr} + \alpha u(t) + d(t) \quad (27)$$

If we substitute Eq (26) into Eq (27),

$$\dot{s}(t) = -\kappa s(t) - \eta \operatorname{sgn}(s(t)) + d(t) \quad (28)$$

From Eq (24),

$$\begin{aligned} s(t) \dot{s}(t) &= s(t) [-\kappa s(t) - \eta \operatorname{sgn}(s(t)) + d(t)] \\ &= -\kappa s(t)^2 - \eta s(t) \operatorname{sgn}(s(t)) + Ds(t) \\ &= -\kappa s(t)^2 - \eta |s(t)| + Ds(t) \end{aligned} \quad (29)$$

So, the system is asymptotically stable in case of  $\eta > D$ .

Although the SMC control has invariance property against the external disturbances and parameter changes, this feature is only valid after the sliding surface is reached. However, before reaching to the sliding surface, the invariance property cannot be guaranteed and the system performance is sensitive to perturbations. One of the best ways to overcome this problem is to use a disturbance observer. The total disturbance which including the disturbances and the parameter variations is estimated by the observer and compensated by the controller.

#### 4. EXTENDED STATE OBSERVER BASED SLIDING MODE CONTROL OF THE SERVO SYSTEM

In this study an extended state observer (ESO) is used as a disturbance observer. The general structure of the proposed Extended State Observer Based Sliding Mode Control strategy is shown in Fig. 3.

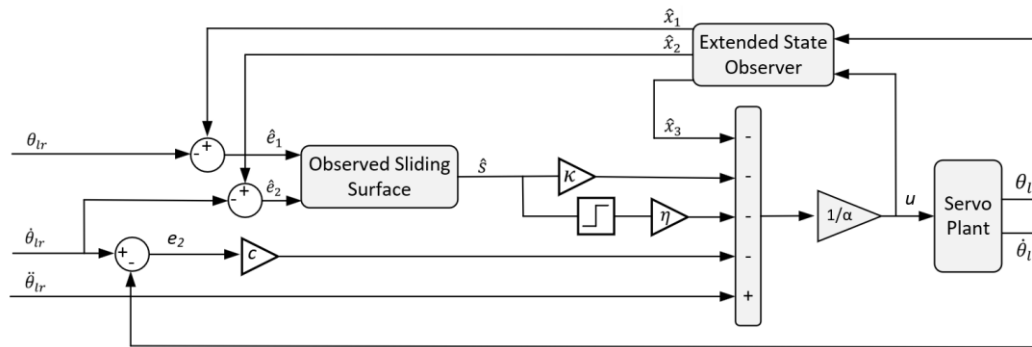


**Figure 3.** Extended state observer-based SMC control scheme

If the system in Eq. (12) is considered as

$$\ddot{\theta}_l = f(\theta, t) + \alpha u(t) \quad (30)$$

where,  $f(\theta, t)$  is a function which includes the external disturbance and uncertain parameters, the state-space model can be written as

$$\begin{aligned} \dot{x}_1(t) &= x_2(t) \\ \dot{x}_2(t) &= f(\theta, t) + \alpha u(t) \end{aligned} \quad (31)$$

If we define an additional state variable as  $x_3(t) = f(\theta, t)$ , the state-space model can be extended as

$$\begin{aligned}
\dot{x}_1(t) &= x_2(t) \\
\dot{x}_2(t) &= f(\theta, t) + \alpha u(t) \\
\dot{x}_3(t) &= \dot{f}(\theta, t)
\end{aligned} \tag{32}$$

Now, the ESO can be designed as

$$\begin{aligned}
\dot{\hat{x}}_1(t) &= \hat{x}_2(t) - \beta_1 \epsilon(t) \\
\dot{\hat{x}}_2(t) &= \hat{x}_3(t) - \beta_2 \epsilon(t) + \alpha_0 u(t) \\
\dot{\hat{x}}_3(t) &= -\beta_3 \epsilon(t)
\end{aligned} \tag{33}$$

where  $\hat{x}_1(t)$ ,  $\hat{x}_2(t)$ ,  $\hat{x}_3(t)$  are the approximated values of  $x_1(t)$ ,  $x_2(t)$ ,  $x_3(t)$  respectively,  $\beta_1, \beta_2, \beta_3$  are the observer gains,  $\epsilon(t) = x_1(t) - \hat{x}_1(t)$  is the approximation error of  $x_1(t)$ . The observer gains  $\beta_1, \beta_2, \beta_3$  can be computed from the characteristic polynomial of the ESO. The observer pole  $\omega_{ESO}$  is usually placed 3 to 10 times to the left of the closed loop pole  $\omega_C$  to ensure that the observer dynamics are fast enough. The respective solutions for  $\beta_{o1}, \beta_{o2}, \beta_{o3}$  are as follows.

$$\omega_{ESO} = (3 - 10)\omega_C, \quad \beta_{o1} = 3\omega_{ESO}, \quad \beta_{o2} = 3\omega_{ESO}^2, \quad \beta_{o3} = \omega_{ESO}^3 \tag{34}$$

The observing sliding surface can be defined as

$$\hat{s}(t) = c \hat{e}_1(t) + \hat{e}_2(t) \tag{35}$$

where  $\hat{e}_1(t) = \hat{x}_1(t) - \theta_{lr}$  and  $\hat{e}_2(t) = \hat{x}_2(t) - \dot{\theta}_{lr}$ . We can select the control signal as

$$u = \frac{1}{\alpha} (\ddot{\theta}_{lr} - \hat{x}_3(t) - c e_2(t) - \kappa \hat{s}(t) - \eta \operatorname{sgn}(\hat{s}(t))) \tag{36}$$

### Stability Proof:

Sliding surface for the system given in Eq. (31) can be selected as,

$$s(t) = c e_1(t) + e_2(t) \tag{37}$$

Derivative of the sliding surface is,

$$\dot{s}(t) = c \dot{e}_1(t) + \dot{e}_2(t) = c e_2(t) + f(\theta, t) - \ddot{\theta}_{lr} + \alpha u(t) \tag{38}$$

If we substitute Eq. (36) into Eq. (38) and Eq. (38) into Eq. (24),

$$\begin{aligned}
\dot{V}(t) &= s[f(\theta, t) - \hat{x}_3(t) + c(e_2(t) - \hat{e}_2(t) - \kappa \hat{s}(t) - \eta \operatorname{sgn}(\hat{s}(t)))] \\
&= (\hat{s} + s - \hat{s})[f(\theta, t) - \hat{x}_3(t) + c(e_2(t) - \hat{e}_2(t) - \kappa \hat{s}(t) - \eta \operatorname{sgn}(\hat{s}(t)))] \\
&= (|f(\theta, t) - \hat{x}_3(t)| + c|e_2(t) - \hat{e}_2(t)|)|\hat{s}(t)| \\
&\quad + (|f(\theta, t) - \hat{x}_3(t)| + c|e_2(t) - \hat{e}_2(t)|)|s(t) - \hat{s}(t)| \\
&\quad - \hat{s}(t) \left[ \kappa (\hat{s}(t) + \eta \operatorname{sgn}(\hat{s}(t))) \right] - |s(t) - \hat{s}(t)| \left[ \kappa (\hat{s}(t) + \eta \operatorname{sgn}(\hat{s}(t))) \right]
\end{aligned} \tag{39}$$

Due to convergence of the ESO,

$$(|f(\theta, t) - \hat{x}_3(t)| + c|e_2(t) - \hat{e}_2(t)|)|\hat{s}(t)| \tag{40}$$

$$+ (|f(\theta, t) - \hat{x}_3(t)| + c|e_2(t) - \hat{e}_2(t)|) |s(t) - \hat{s}(t)| - |s(t) - \hat{s}(t)| \left[ \kappa \left( \hat{s}(t) + \eta \operatorname{sgn}(\hat{s}(t)) \right) \right] \cong 0$$

is bounded and close to zero. So,

$$\dot{V}(t) = -\hat{s}(t) \left( \kappa \left( \hat{s}(t) + \eta \operatorname{sgn}(\hat{s}(t)) \right) \right) = -\kappa \hat{s}(t)^2 - \eta |\hat{s}(t)| < 0 \quad (41)$$

## 5. RESULTS AND DISCUSSION

The performance of the proposed ESOSMC controller was examined for five different conditions according to different disturbance inputs affecting the system. The control results of the ESOSMC are compared with the traditional PD and SMC control results to evaluate its effectiveness. A square signal with 0.4 rad amplitude and 0.4 Hz frequency was used as reference input. The parameters of the SRV02 rotary servo unit are given in Table 1 and the parameters of the PID controller are taken as  $k_p = 1.79$ ,  $k_d = 4.66 \times 10^{-4}$  and  $k_i = 0$ . These values are the optimum values determined by the manufacturer. The controller parameters are chosen as,  $c = 85$ ,  $\eta = 30$  and  $\kappa = 20$  for the SMC and  $c = 85$ ,  $\eta = 1$ ,  $\kappa = 20$  and  $\omega_o = 100$  for the ESOSMC. The signum function in the control signal has been replaced by the saturation function to reduce the chattering.

**Table 1.** Parameters of the SRV02 rotary servo unit

Symbols	Definitions	Value
$J_m$	Moment of inertia of the motor shaft	$4.6 \times 10^{-07}$ (kgm <sup>2</sup> )
$J_l$	Moment of inertia of the load shaft	$1.6 \times 10^{-05}$ (kgm <sup>2</sup> )
$J_{eq}$	Equivalent moment of inertia	$9.8 \times 10^{-05}$ (kgm <sup>2</sup> )
$B_{eq}$	Equivalent Viscous Damping Coefficient	$15 \times 10^{-05}$ (Nms/rad)
$K_g$	Gear ratio	14
$k_t$	Current-torque constant	0.0077 (Nm/A)
$k_m$	Back-emf constant	0.0077 (Vs/rad)
$\eta_g$	Gearbox efficiency	0.9
$\eta_m$	Motor efficiency	0.69
$R_m$	Armature resistance	2.6 (ohm)

**1<sup>st</sup> condition:** The performances of the controllers were evaluated under ideal system conditions without parameter variations and disturbances. The controller responses and the control voltages are given in Fig.4 and Fig.5 respectively. As seen in Figure 4, ESOSMC gives better results than other controllers in terms of response speed. Also, an overshoot occurred in the PD control response and a small steady-state error was observed in the traditional SMC response.

**2<sup>nd</sup> condition:** The equivalent moment of inertia of the servo system was increased by 500% by connecting a load to the motor shaft in order to examine the robustness of the controllers against the parameter variations. The controller responses and the control voltages are given in Fig.6 and Fig.7 respectively. Accordingly, it is seen that the SMC and the ESOSMC are completely insensitive to parameter variations, while the PD controller is greatly affected and its response shows large deviations from the desired response.

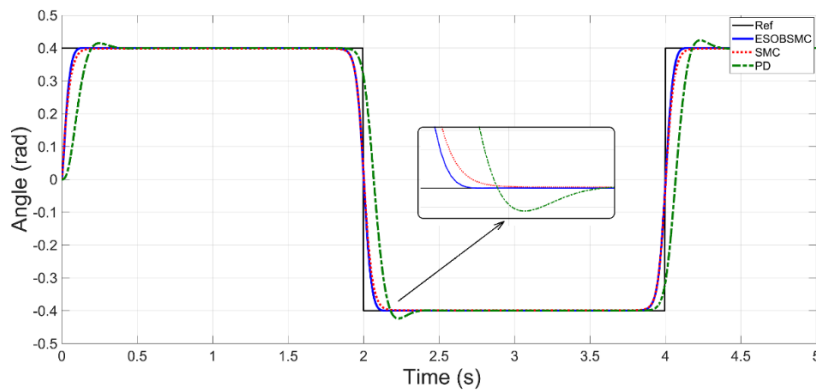


**Figure 4.** Controller responses in case of ideal conditions (no parameter variations or disturbance)

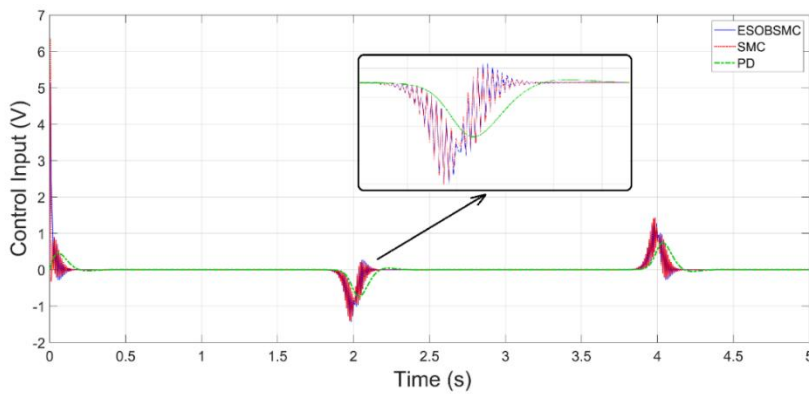


**Figure 5.** Controller voltages in case of ideal conditions (no parameter variations or disturbance)

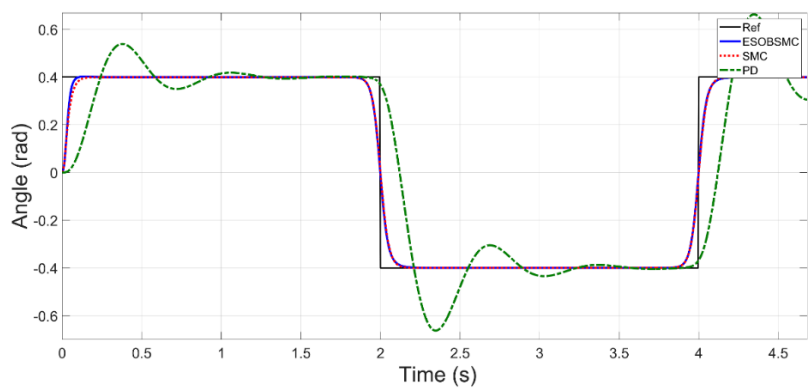


**Figure 6.** Controller responses in case the equivalent moment of inertia is increased by 500%

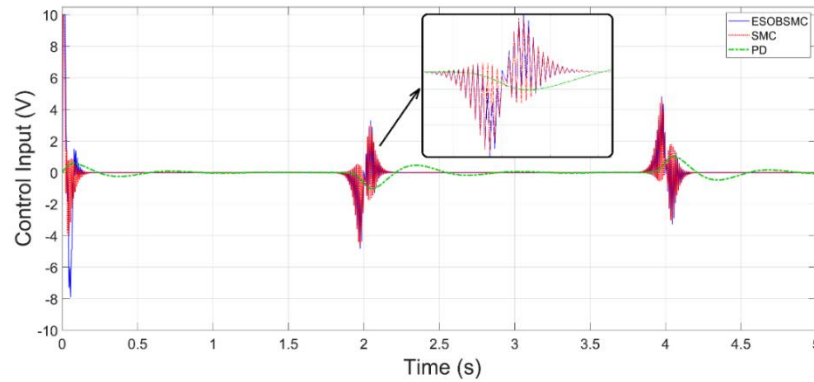


**Figure 7.** Controller voltages in case the equivalent moment of inertia is increased by 500%

**3<sup>rd</sup> condition:** A time dependent  $d_1(t) = 25 \sin(5t)$  disturbance input was applied to the input channel of the system in order to examine the disturbance rejection performances of the controllers against the matched disturbances. The controller responses and the control voltages are given in Fig.8 and Fig.9 respectively. It can be clearly seen from Fig. 8 that the PD control is highly sensitive to matched disturbances and its response shows large deviations from the desired response. As mentioned earlier, the traditional SMC control has invariance property against the matching disturbances. In accordance with this, the SMC control has generally given a successful response against the matched disturbance except some deviations shown in the zoomed part of the Fig. 8. On the other hand, it is also seen that the proposed ESOSMC controller has provided a better disturbance rejection ability against the matched disturbances than SMC.

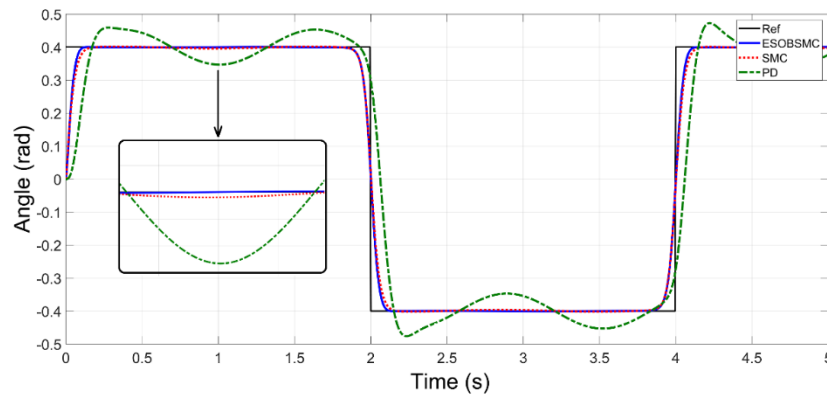


**Figure 8.** Controller responses in case of  $d_1 = 25 \sin(5t)$  matched disturbance input

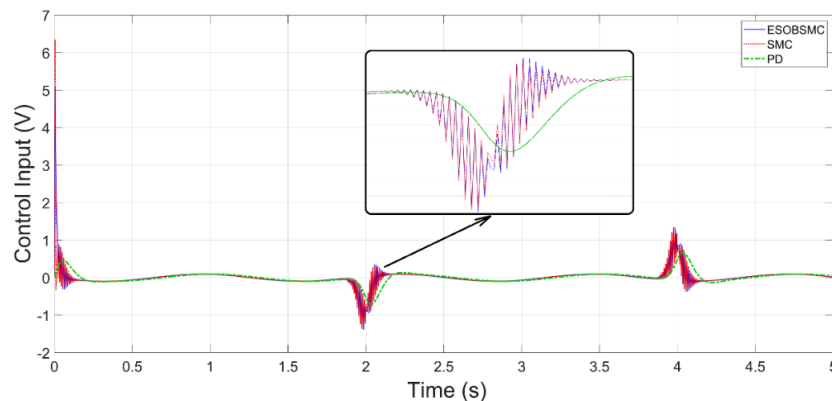


**Figure 9.** Controller voltages in case of  $d_1 = 25 \sin(5t)$  matched disturbance input

**4<sup>th</sup> condition:** A time dependent  $d_1(t) = 0.5 \sin(5t)$  disturbance input was applied directly to system in order to examine the disturbance rejection performances of the controllers against the mismatched disturbances. The controller responses and the control voltages are given in Fig. 10 and Fig. 11 respectively. As mentioned earlier, although the traditional SMC control is insensitive to matched disturbances, this feature is not valid to mismatched disturbances. It can be seen from Fig. 10; both the PD and SMC control are extremely sensitive to mismatched disturbances and the controller responses have deviated considerably from the desired response. On the other hand, it can be clearly seen that the proposed ESOSMC controller is completely insensitive to mismatched disturbances and it has provided a perfect disturbance rejection ability.

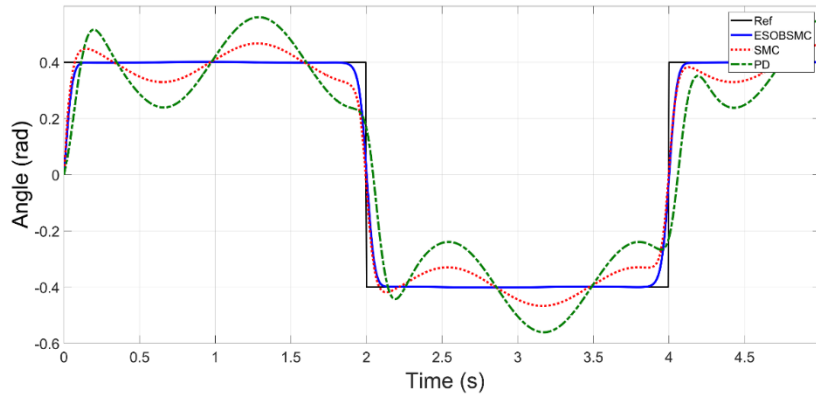


**Figure 10.** Controller responses in case of  $d_2 = 0.5 \sin(5t)$  mismatched disturbance input

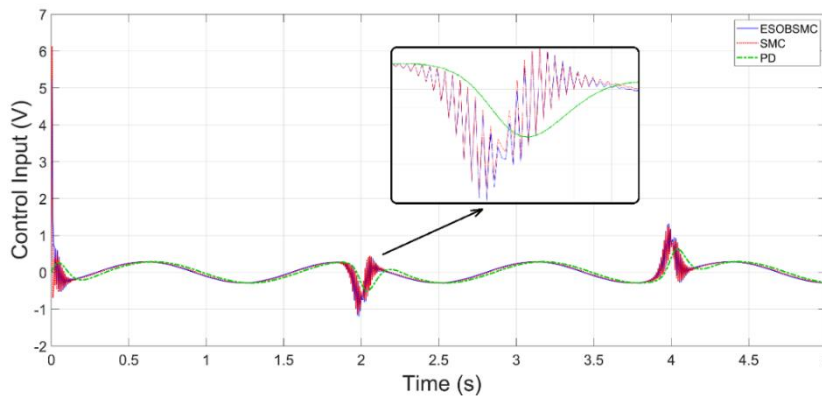


**Figure 11.** Controller voltages in case of  $d_2 = 0.5 \sin(5t)$  mismatched disturbance input

**5<sup>th</sup> condition:** As the last condition, the parameter variation and the matched and unmatched disturbance inputs given in the previous conditions were applied to the system at the same time. The controller responses and the control voltages are given in Fig. 12 and Fig. 13 respectively. It is clearly seen from Figure 12 that the proposed ESOSMC controller can offer a superior performance compared to other controllers in terms of both response speed and disturbance rejection, even if parameter changes and matched and unmatched disturbances affect the system at the same time.

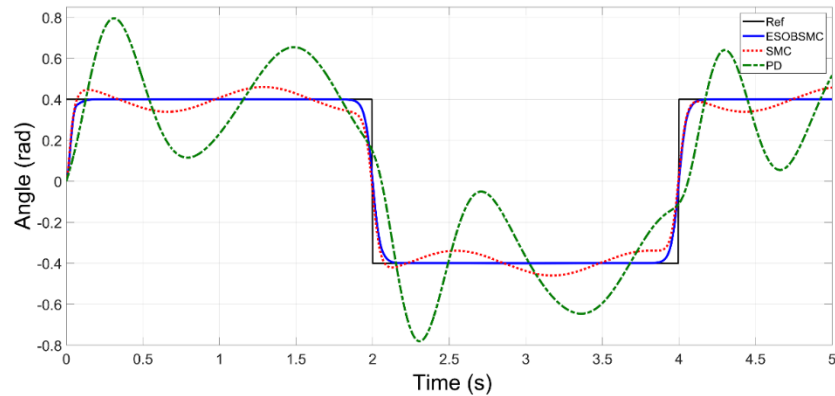


**Figure 12.** Controller responses in case of increasing the equivalent moment of inertia by 500% and at the same time applying  $d_1 = 25 \sin(5t)$  matched disturbance and  $d_2 = 0.5 \sin(5t)$  unmatched disturbance inputs to the system

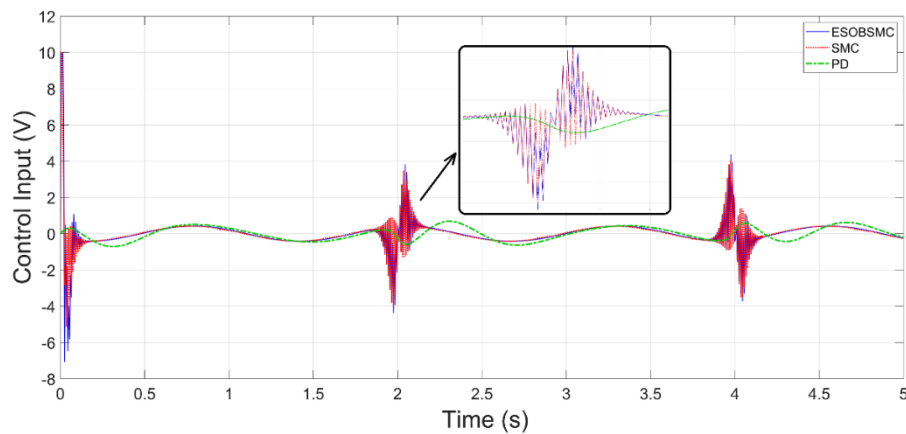


**Figure 13.** Controller voltages in case of increasing the equivalent moment of inertia by 500% and at the same time applying  $d_1 = 25 \sin(5t)$  matched disturbance and  $d_2 = 0.5 \sin(5t)$  unmatched disturbance inputs to the system

On the other hand, while the PD control provides a smooth control signal for all conditions, both SMC and the proposed ESOSMC controllers showed chattering, although it is not critical level. The amount of the chattering in control signal was slightly reduced by using the saturation function instead of the sign function, but it is seen that the extended state observer cannot provide a significant improvement in the chattering phenomenon.

## 6. CONCLUSION

In this study, extended state observer-based sliding mode control scheme has been proposed for precise position control of a rotary servo system. The proposed control scheme is tested via simulation studies for five different conditions consisted of different uncertainties and disturbances and its performance were compared with the PD controller and the traditional SMC controller. The simulation results showed that the PD control is sensitive to parameter changes and disturbances while the SMC control is sensitive to mismatched disturbances. However, it has been seen that the proposed control scheme is much more successful than the PD and SMC control in terms of both the response speed and the ability to reject disturbances including mismatched disturbances.

## 7. REFERENCES

- Baik, I. C., Kim, K. H., & Youn, M. J., 2000, "Robust nonlinear speed control of PM synchronous motor using boundary layer integral sliding mode control technique", *IEEE Transactions on Control Systems Technology*, 8(1), 47-54.
- Bao, G., Zhang, Q., Lu, J., Xun, Y., & Yang, Q., 2010, "Sliding-mode position control of robot joint based on self-adaptive parameters adjusting", In *2010 IEEE International Conference on Robotics and Biomimetics* (pp. 478-483). IEEE.
- Bartolini, G., Ferrara, A., & Usai, E., 1998, "Chattering avoidance by second-order sliding mode control", *IEEE Transactions on automatic control*, 43(2), 241-246.
- Chang, Y., 2009, "Adaptive sliding mode control of multi-input nonlinear systems with perturbations to achieve asymptotical stability", *IEEE Transactions on automatic control*, 54(12), 2863-2869.
- Cheon, J. W., Choi, S. B., Song, H. J., & Ham, J. H., 2004, "Position control of an AC servo motor using sliding mode controller with disturbance estimator", *International journal of precision engineering and manufacturing*, 5(4), 14-20.
- Ha, Q. P., Nguyen, Q. H., Rye, D. C., & Durrant-Whyte, H. F., 2001, "Fuzzy sliding-mode controllers with applications", *IEEE Transactions on industrial electronics*, 48(1), 38-46.
- Hou, L., Wang, L., & Wang, H., 2017, "SMC for systems with matched and mismatched uncertainties and disturbances based on NDOB", *Acta Automatica Sinica*, 43(7), 1257-1264.
- Kachroo, P., & Tomizuka, M., 1996, "Chattering reduction and error convergence in the sliding-mode control of a class of nonlinear systems", *IEEE Transactions on automatic control*, 41(7), 1063-1068.
- Levant, A., 2003, "Higher-order sliding modes, differentiation and output-feedback control", *International journal of Control*, 76(9-10), 924-941.
- Li, H. Y., & Hu, Y. A., 2011, "Robust sliding-mode backstepping design for synchronization control of cross-strict feedback hyperchaotic systems with unmatched uncertainties", *Communications in Nonlinear Science and Numerical Simulation*, 16(10), 3904-3913.
- Liu, X., Wu, Y., Deng, Y., & Xiao, S., 2014, "A global sliding mode controller for missile electromechanical actuator servo system", *Proceedings of the Institution of Mechanical Engineers, Part G: Journal of Aerospace Engineering*, 228(7), 1095-1104.
- Nguyen, D. G., Tran, D. T., & Ahn, K. K., 2021, "Disturbance Observer-Based Chattering-Attenuated Terminal Sliding Mode Control for Nonlinear Systems Subject to Matched and Mismatched Disturbances", *Applied Sciences*, 11(17), 8158.
- Rubagotti, M., Estrada, A., Castañón, F., Ferrara, A., & Fridman, L., 2011, "Integral sliding mode control for nonlinear systems with matched and unmatched perturbations", *IEEE Transactions on Automatic Control*, 56(11), 2699-2704.
- Shao, K., Zheng, J., Wang, H., Xu, F., Wang, X., & Liang, B., 2021, "Recursive sliding mode control with adaptive disturbance observer for a linear motor positioner", *Mechanical Systems and Signal Processing*, 146, 107014.
- Shi, S. L., Li, J. X., & Fang, Y. M., 2018, "Extended-state-observer-based chattering free sliding mode control for nonlinear systems with mismatched disturbance", *IEEE Access*, 6, 22952-22957.
- Tseng, M. L., & Chen, M. S., 2010, "Chattering reduction of sliding mode control by low-pass filtering the control signal", *Asian Journal of control*, 12(3), 392-398.
- Wang, A., Jia, X., & Dong, S., 2013, "A new exponential reaching law of sliding mode control to improve performance of permanent magnet synchronous motor", *IEEE Transactions on Magnetics*, 49(5), 2409-2412.
- Wang, H., Li, S., Lan, Q., Zhao, Z., & Zhou, X., 2017, "Continuous terminal sliding mode control with extended state observer for PMSM speed regulation system", *Transactions of the Institute of Measurement and Control*, 39(8), 1195-1204.
- Wang, L., Chai, T., & Zhai, L., 2009, "Neural-network-based terminal sliding-mode control of robotic manipulators including actuator dynamics", *IEEE Transactions on Industrial Electronics*, 56(9), 3296-3304.

- Wang, S., Tao, L., Chen, Q., Na, J., & Ren, X., 2020, "USDE-based sliding mode control for servo mechanisms with unknown system dynamics", *IEEE/ASME Transactions on Mechatronics*, 25(2), 1056-1066.
- Zheng, J., Wang, H., Man, Z., Jin, J., & Fu, M., 2014, "Robust motion control of a linear motor positioner using fast nonsingular terminal sliding mode", *IEEE/ASME Transactions on Mechatronics*, 20(4), 1743-1752.